# Substructure Finite Element Model Updating of a Space Frame Structure by Minimization of Modal Dynamic Residual

Dapeng Zhu, Xinjun Dong, Yang Wang, *Member, IEEE*

***Abstract*—This research investigates a substructure model updating approach for large-scale structures. The approach requires instrumentation in only part of a large structure (i.e. a substructure), and is capable of updating the model parameters for the substructure. Prior to updating, the entire structural model is divided into the substructure (currently being instrumented and to be updated) and the residual structure. Craig-Bampton transform is adopted to condense the residual structure using a limited number of dominant mode shapes, while the substructure remains at high resolution. To update the condensed structural model, physical parameters in the substructure and modal parameters of the residual structure are chosen as optimization variables; minimization of the modal dynamic residual is chosen as the optimization objective. A space frame structure, simulating a pedestrian bridge on Georgia Tech campus, is adopted to validate the proposed approach. About a quarter of the bridge model is selected as the substructure to be instrumented and updated. For comparison, a conventional model updating approach, which minimizes modal property differences, is also adopted to update the substructure model. The results show that the proposed substructure updating approach, which minimizes modal dynamic residual, gives better accuracy compared to the conventional approach.**

## I. INTRODUCTION

Though significant advances have been achieved in finite element (FE) modeling of engineering structures, differences usually exist between predictions of an FE model and experimental measurements from the actual structure. The discrepancies are mainly caused by complexity of the actual structure and limitations in FE modeling. For higher simulation accuracy, it is essential to update the finite element model based on experimental measurements on the actual structure. Numerous FE model updating algorithms have been developed and practically applied in the past few decades [1]. Most algorithms can be categorized into two groups, i.e. frequency-domain approaches and time-domain approaches. Frequency-domain approaches update an FE model using frequency-domain structural characteristics extracted from experimental measurements, such as vibration modes [2, 3]. On the other hand, time-domain approaches directly utilize measured time histories for model updating [4, 5]. Nevertheless, most of the existing algorithms operate on an entire structural model with very large amount of degrees of freedom (DOFs), thus they may suffer significant computational challenges and convergence problem.

In order to address the difficulties, some research activities have been devoted to substructure model updating, which operates on part of a large structure with relatively small number of DOFs. Among frequency-domain approaches, Link adopts Craig-Bampton transform for substructure modeling, and updates the substructure model by minimizing difference between simulated and experimental modal properties [6, 7]. In [8], interface force vectors are estimated using multiple sets of measurement; the difference between multiple estimations is minimized with genetic algorithms for substructure model updating. Other researchers adopt frequency spectra for substructure identification, by minimizing difference between simulated and experimental acceleration spectra in certain frequency range [9, 10]. Among time-domain approaches, the substructure model is always built by considering interface coupling effects as known/unknown external load. For example, some algorithms only update the physical parameters inside the substructure by assuming interface dynamic force is known or can be pre-estimated [11-13]. Recently, the sequential nonlinear least square estimation (SNLSE) method has been explored for substructure model updating [14]. The unknown interface coupling terms are treated as unknown forces, and updated in each time step sequentially with state variables and system parameters. Furthermore, Yuen and Katafygiotis present a substructure identification procedure using Bayesian theorem, without requiring interface measurements or excitation measurements [15].

This research investigates substructure updating using frequency domain data. The entire structural model is divided into the substructure (currently being instrumented and to be updated) and the residual structure. Craig-Bampton transform is adopted to condense the residual structure using a limited number of dominant mode shapes, while the substructure model remains at high resolution. To update the condensed structural model, physical parameters in the substructure and modal parameters of the residual structure are chosen as optimization variables, and minimization of the modal dynamic residual is chosen as the optimization objective. An iterative linearization procedure is adopted for efficiently solving the optimization problem [3, 16, 17]. The approach is previously validated with a few 2D structural models. This research attempts to validate the approach with a more complicated 3D frame structure.

*Research supported by National Science Foundation (CMMI-1150700 and CMMI-1041607), the Research and Innovative Technology Administration of US DOT (#DTRT12GUTC12) and Georgia DOT (#RP12-21)

Dapeng Zhu, Xinjun Dong, Yang Wang are with the School of Civil and Environmental Engineering, Georgia Institute of Technology, Atlanta, GA 30332 USA (corresponding author: Yang Wang. email : yang.wang@ce.gatech.edu; phone: +1(404) 894-1851; fax: +1(404)385-0337)

The rest of the paper is organized as follows. Section II presents the formulation of substructure modeling and model updating through modal dynamic residual approach. Section III describes numerical validations using a space frame structure. The performance of the proposed approach is compared with a conventional updating procedure that minimizes experimental and simulated modal property differences. Finally, a summary and discussion are provided.

## II. Substructure Modeling and Updating

This section presents the basic formulation for substructure updating. Section A describes substructure modeling strategy following Craig-Bampton transform. Section B describes substructure model updating through minimization of modal dynamic residual.

### A. Substructure modeling

Figure 1 illustrates the substructure modeling strategy. Subscripts *s*, *i*, and *r* are used to denote DOFs associated with the substructure being analyzed, the interface nodes, and the residual structure, respectively. The block-bidiagonal structural stiffness and mass matrices, **K** and **M**, can be assembled using original DOFs $\mathbf{x} = [\mathbf{x}_s \quad \mathbf{x}_i \quad \mathbf{x}_r]^{\mathrm{T}}$.

$$\mathbf{K} = \begin{bmatrix} \begin{bmatrix} \mathbf{K}_S \end{bmatrix} & \mathbf{0} \\ & \mathbf{0} \\ \mathbf{0} \quad \mathbf{0} & \mathbf{0} \end{bmatrix} + \begin{bmatrix} \mathbf{0} & \mathbf{0} \quad \mathbf{0} \\ \mathbf{0} & \\ \mathbf{0} & \begin{bmatrix} \mathbf{K}_R \end{bmatrix} \end{bmatrix} = \begin{bmatrix} \begin{bmatrix} \mathbf{K}_{ss} & \mathbf{K}_{si} \\ \mathbf{K}_{is} & \mathbf{K}_{ii}^S \end{bmatrix} & \begin{matrix} \mathbf{0} \\ \mathbf{0} \end{matrix} \\ \begin{matrix} \mathbf{0} & \mathbf{0} \end{matrix} & \mathbf{0} \end{bmatrix} + \begin{bmatrix} \mathbf{0} & \begin{matrix} \mathbf{0} & \mathbf{0} \end{matrix} \\ \begin{matrix} \mathbf{0} \\ \mathbf{0} \end{matrix} & \begin{bmatrix} \mathbf{K}_{ii}^R & \mathbf{K}_{ir} \\ \mathbf{K}_{ri} & \mathbf{K}_{rr} \end{bmatrix} \end{bmatrix} \tag{1}$$

$$\mathbf{M} = \begin{bmatrix} \begin{bmatrix} \mathbf{M}_S \end{bmatrix} & \mathbf{0} \\ & \mathbf{0} \\ \mathbf{0} \quad \mathbf{0} & \mathbf{0} \end{bmatrix} + \begin{bmatrix} \mathbf{0} & \mathbf{0} \quad \mathbf{0} \\ \mathbf{0} & \\ \mathbf{0} & \begin{bmatrix} \mathbf{M}_R \end{bmatrix} \end{bmatrix} = \begin{bmatrix} \begin{bmatrix} \mathbf{M}_{ss} & \mathbf{M}_{si} \\ \mathbf{M}_{is} & \mathbf{M}_{ii}^S \end{bmatrix} & \begin{matrix} \mathbf{0} \\ \mathbf{0} \end{matrix} \\ \begin{matrix} \mathbf{0} & \mathbf{0} \end{matrix} & \mathbf{0} \end{bmatrix} + \begin{bmatrix} \mathbf{0} & \begin{matrix} \mathbf{0} & \mathbf{0} \end{matrix} \\ \begin{matrix} \mathbf{0} \\ \mathbf{0} \end{matrix} & \begin{bmatrix} \mathbf{M}_{ii}^R & \mathbf{M}_{ir} \\ \mathbf{M}_{ri} & \mathbf{M}_{rr} \end{bmatrix} \end{bmatrix} \tag{2}$$

Here $\mathbf{K}_S$ and $\mathbf{M}_S$ denote entries of the stiffness and mass matrices corresponding to the substructure; $\mathbf{K}_R$ and $\mathbf{M}_R$ denote entries corresponding to the residual structure; $\mathbf{K}_{ii}^S$ and $\mathbf{M}_{ii}^S$ denote the entries at the interface DOFs and contributed by the substructure; $\mathbf{K}_{ii}^R$ and $\mathbf{M}_{ii}^R$ denote entries at the interface DOFs and contributed by the residual structure. For simplicity, the formulation is provided neglecting damping, although the substructure updating approach can consider damping upon some modification.

The dynamic behavior of the residual structure can be approximated using Craig-Bampton formulation [6]. The DOFs of the residual structure, $\mathbf{x}_r \in \mathbb{R}^{n_r}$, are approximated by a linear combination using interface DOFs, $\mathbf{x}_i \in \mathbb{R}^{n_i}$, and modal coordinates of the residual structure, $\mathbf{q}_r \in \mathbb{R}^{n_q}$.

$$\mathbf{x}_r \approx \mathbf{T}\mathbf{x}_i + \mathbf{\Phi}_r \mathbf{q}_r \tag{3}$$

Here $\mathbf{T} = -\mathbf{K}_{rr}^{-1}\mathbf{K}_{ri}$ is the Guyan static condensation matrix; $\mathbf{\Phi}_r = \left[\boldsymbol{\varphi}_1, \ldots, \boldsymbol{\varphi}_{n_q}\right]$ represents the mode shapes of the residual structure with interface DOFs fixed. The eigenvalue equation providing the mode shapes, $\boldsymbol{\varphi}_j$ ($j$=1, ..., $n_q$), and modal frequencies, $\omega_{r,j}$, can be written as

$$\left(-\omega_{r,j}{}^2\mathbf{M}_{rr} + \mathbf{K}_{rr}\right)\boldsymbol{\varphi}_j = 0, \qquad j = 1, \ldots, n_q \tag{4}$$

Although the size of the residual structure may be large, the number of modal coordinates, $n_q$, can be chosen as relatively small to reflect the first few dominant mode shapes only (i.e. $n_q << n_r$). The coordinate transformation is rewritten in vector form as:

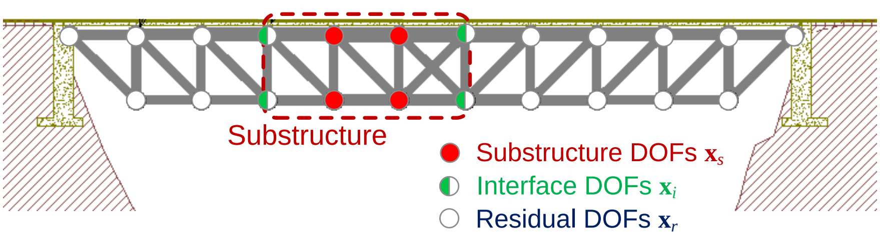


Figure 1. Illustration of substructure modeling strategy.

$$\begin{bmatrix} \mathbf{x}_i \\ \mathbf{x}_r \end{bmatrix} \approx \mathbf{\Gamma} \begin{bmatrix} \mathbf{x}_i \\ \mathbf{q}_r \end{bmatrix}, \text{ where } \quad \mathbf{\Gamma} = \begin{bmatrix} \mathbf{I} & \\ \mathbf{T} & \mathbf{\Phi}_r \end{bmatrix} \tag{5}$$

Suppose $\tilde{\mathbf{K}}_R$ and $\tilde{\mathbf{M}}_R$ denote the new stiffness and mass matrices of the residual structure after transformation:

$$\tilde{\mathbf{K}}_R = \mathbf{\Gamma}^{\mathrm{T}} \mathbf{K}_R \mathbf{\Gamma} \qquad \tilde{\mathbf{M}}_R = \mathbf{\Gamma}^{\mathrm{T}} \mathbf{M}_R \mathbf{\Gamma} \tag{6}$$

Link described a model updating method for both the substructure and the residual structure [7]. The substructure model is updated as

$$\mathbf{K}_S = \mathbf{K}_{S0} + \sum_{j=1}^{n_\alpha} \alpha_j \mathbf{K}_{S0,j} \qquad \mathbf{M}_S = \mathbf{M}_{S0} + \sum_{j=1}^{n_\beta} \beta_j \mathbf{M}_{S0,j} \tag{7}$$

where $\mathbf{K}_{S0}$ and $\mathbf{M}_{S0}$ are the stiffness and mass matrices of the substructure and used as initial starting point in the model updating; $\alpha_j$ and $\beta_j$ correspond to physical system parameters to be updated, such as elastic modulus and density of each substructure element; $n_\alpha$ and $n_\beta$ represent the total number of corresponding parameters to be updated; $\mathbf{K}_{S0,j}$ and $\mathbf{M}_{S0,j}$ are constant matrices determined by the type and location of these parameters. Subscript “0” will be used hereinafter to denote variables associated with the initial structural model, which serves as the starting point for model updating.

The matrices of the condensed residual structural model, $\tilde{\mathbf{K}}_R$ and $\tilde{\mathbf{M}}_R$ in Eq.(6), each contains $(n_i + n_q) \times (n_i + n_q)$ number of entries. Assuming that physical changes in the residual structure do not significantly alter the generalized eigenvectors of $\tilde{\mathbf{K}}_R$ and $\tilde{\mathbf{M}}_R$, only $(n_i + n_q)$ number of modal parameters are selected as updating parameters for each condensed matrix of the residual structural model :

$$\tilde{\mathbf{K}}_R = \tilde{\mathbf{K}}_{R0} + \sum_{j=1}^{n_i+n_q} \zeta_j \tilde{\mathbf{K}}_{R0,j} \qquad \tilde{\mathbf{M}}_R = \tilde{\mathbf{M}}_{R0} + \sum_{j=1}^{n_i+n_q} \eta_j \tilde{\mathbf{M}}_{R0,j} \tag{8}$$

where $\zeta_j$ and $\eta_j$ are the modal parameters to be updated; $\tilde{\mathbf{K}}_{R0}$ and $\tilde{\mathbf{M}}_{R0}$ are the initial stiffness and mass matrices of the condensed residual structure model; $\tilde{\mathbf{K}}_{R0,j}$ and $\tilde{\mathbf{M}}_{R0,j}$ represent the constant correction matrices formulated using modal back-transform:

$$\tilde{\mathbf{K}}_{R0,j} = \boldsymbol{\varphi}_{R0,j}^{l} \omega_{R0,j}^{2} \boldsymbol{\varphi}_{R0,j}^{l,\mathrm{T}} \qquad \tilde{\mathbf{M}}_{R0,j} = \boldsymbol{\varphi}_{R0,j}^{l} \boldsymbol{\varphi}_{R0,j}^{l,\mathrm{T}} \tag{9}$$

where

$$\begin{bmatrix} \boldsymbol{\varphi}_{R0,1}^{l} & \cdots & \boldsymbol{\varphi}_{R0,n_i+n_q}^{l} \end{bmatrix} = \mathbf{\Phi}_{R0}^{-\mathrm{T}} = \begin{bmatrix} \boldsymbol{\varphi}_{R0,1} & \cdots & \boldsymbol{\varphi}_{R0,n_i+n_q} \end{bmatrix}^{-\mathrm{T}} \tag{10}$$

$\omega_{R0,j}^2$ and $\boldsymbol{\varphi}_{R0,j}$ are the $j$-th generalized eigenvalue and eigenvector of the initial transformed residual structural matrices:

$$\mathbf{\Phi}_{R0}^{\mathrm{T}} \tilde{\mathbf{M}}_{R0} \mathbf{\Phi}_{R0} = \mathbf{I} \qquad \mathbf{\Phi}_{R0}^{\mathrm{T}} \tilde{\mathbf{K}}_{R0} \mathbf{\Phi}_{R0} = \mathrm{diag}(\omega_{R0,1}^2, \cdots, \omega_{R0,(n_q+n_i)}^2) \tag{11}$$

Using all model matrices to be updated, i.e. Eq. (7) for substructure and Eq. (8) for residual structure, the condensed entire structural model with reduced DOFs, $\begin{bmatrix} \mathbf{x}_s & \mathbf{x}_i & \mathbf{q}_r \end{bmatrix}^{\mathrm{T}}$, can be updated with variables $\alpha_j$, $\beta_j$, $\zeta_j$ and $\eta_j$. For brevity, these variables will be referred to in vector form as $\boldsymbol{\alpha} \in \mathbb{R}^{n_\alpha}$ , $\boldsymbol{\beta} \in \mathbb{R}^{n_\beta}$ , $\boldsymbol{\zeta} \in \mathbb{R}^{n_i+n_q}$ and $\boldsymbol{\eta} \in \mathbb{R}^{n_i+n_q}$ .

$$\tilde{\mathbf{K}} = \tilde{\mathbf{K}}_0 + \sum_{j=1}^{n_\alpha} \alpha_j \begin{bmatrix} \begin{bmatrix} \mathbf{K}_{S0,j} \end{bmatrix} & \mathbf{0} \\ & \mathbf{0} \\ \mathbf{0} \quad \mathbf{0} & \mathbf{0} \end{bmatrix} + \sum_{j=1}^{n_i+n_q} \zeta_j \begin{bmatrix} \mathbf{0} & \mathbf{0} \quad \mathbf{0} \\ \mathbf{0} & \\ \mathbf{0} & \begin{bmatrix} \tilde{\mathbf{K}}_{R0,j} \end{bmatrix} \end{bmatrix} = \tilde{\mathbf{K}}_0 + \sum_{j=1}^{n_\alpha} \alpha_j \mathbf{S}_{\alpha,j} + \sum_{j=1}^{n_i+n_q} \zeta_j \mathbf{S}_{\zeta,j} \tag{12}$$

$$\tilde{\mathbf{M}} = \tilde{\mathbf{M}}_0 + \sum_{j=1}^{n_\beta} \beta_j \begin{bmatrix} \begin{bmatrix} \mathbf{M}_{S0,j} \end{bmatrix} & \mathbf{0} \\ & \mathbf{0} \\ \mathbf{0} \quad \mathbf{0} & \mathbf{0} \end{bmatrix} + \sum_{j=1}^{n_i+n_q} \eta_j \begin{bmatrix} \mathbf{0} & \mathbf{0} \quad \mathbf{0} \\ \mathbf{0} & \\ \mathbf{0} & \begin{bmatrix} \tilde{\mathbf{M}}_{R0,j} \end{bmatrix} \end{bmatrix} = \tilde{\mathbf{M}}_0 + \sum_{j=1}^{n_\alpha} \beta_j \mathbf{S}_{\beta,j} + \sum_{j=1}^{n_i+n_q} \eta_j \mathbf{S}_{\eta,j} \tag{13}$$

where $\mathbf{S}_{\alpha,j}$ , $\mathbf{S}_{\beta,j}$ , $\mathbf{S}_{\zeta,j}$ and $\mathbf{S}_{\eta,j}$ represent the constant sensitivity matrices corresponding to variables $\alpha_j$, $\beta_j$, $\zeta_j$ and $\eta_j$, respectively.

*B. Substructure model updating through minimization of modal dynamic residual*

To update the substructure model, a modal dynamic residual approach is proposed in this study. The model updating approach attempts to minimize modal dynamic residual of the generalized eigenvalue equation.

$$\begin{array}{ll} \underset{\boldsymbol{\alpha},\boldsymbol{\beta},\boldsymbol{\zeta},\boldsymbol{\eta},\boldsymbol{\psi}_{\mathrm{u}}}{\text{minimize}} & \sum_{j=1}^{n_{\mathrm{m}}} \left\| \left( \tilde{\mathbf{K}}(\boldsymbol{\alpha},\boldsymbol{\zeta}) - \omega_j^2 \tilde{\mathbf{M}}(\boldsymbol{\beta},\boldsymbol{\eta}) \right) \begin{Bmatrix} \boldsymbol{\psi}_{\mathrm{m},j} \\ \boldsymbol{\psi}_{\mathrm{u},j} \end{Bmatrix} \right\|^2 \\ \text{subject to} & \boldsymbol{\alpha}_L \le \boldsymbol{\alpha} \le \boldsymbol{\alpha}_U; \quad \boldsymbol{\beta}_L \le \boldsymbol{\beta} \le \boldsymbol{\beta}_U; \quad \boldsymbol{\zeta}_L \le \boldsymbol{\zeta} \le \boldsymbol{\zeta}_U; \quad \boldsymbol{\eta}_L \le \boldsymbol{\eta} \le \boldsymbol{\eta}_U \end{array} \tag{14}$$

where $\|\bullet\|$ denotes any vector norm; $n_{\mathrm{m}}$ denotes the number of measured modes from experiments; $\omega_j$ denotes the $j$-th modal frequency extracted from experimental data; $\boldsymbol{\psi}_{\mathrm{m},j}$ denotes the entries in the $j$-th mode shape that correspond to measured (instrumented) DOFs; $\boldsymbol{\psi}_{\mathrm{u},j}$ corresponds to unmeasured DOFs; $\boldsymbol{\alpha}$, $\boldsymbol{\beta}$, $\boldsymbol{\zeta}$ and $\boldsymbol{\eta}$ are the system parameters to be updated (see Eq. (12) and (13)); $\boldsymbol{\alpha}_L$, $\boldsymbol{\beta}_L$, $\boldsymbol{\zeta}_L$ and $\boldsymbol{\eta}_L$ denote the lower bounds for vectors $\boldsymbol{\alpha}$, $\boldsymbol{\beta}$, $\boldsymbol{\zeta}$ and $\boldsymbol{\eta}$, respectively; $\boldsymbol{\alpha}_U$, $\boldsymbol{\beta}_U$, $\boldsymbol{\zeta}_U$ and $\boldsymbol{\eta}_U$ denote the upper bounds for vectors $\boldsymbol{\alpha}$, $\boldsymbol{\beta}$, $\boldsymbol{\zeta}$ and $\boldsymbol{\eta}$, respectively. Note that the sign "≤" in Eq. (14) is overloaded to represent element-wise inequality.

In summary, $\omega_j$ and $\boldsymbol{\psi}_{\mathrm{m},j}$ are extracted using experimental data from the sensors deployed on the substructure and interface DOFs at high density, and thus, are constant in the optimization problem. The optimization variables are $\boldsymbol{\alpha}$, $\boldsymbol{\beta}$, $\boldsymbol{\zeta}$, $\boldsymbol{\eta}$ and $\boldsymbol{\psi}_{\mathrm{u}}$. Eq. (14) leads to a complex nonlinear optimization problem that is generally difficult to solve. However, if mode shapes at unmeasured DOFs, $\boldsymbol{\psi}_{\mathrm{u}}$, were known, Eq. (14) becomes a convex optimization problem[17, 18]. The optimization variables are system parameters ($\boldsymbol{\alpha}$, $\boldsymbol{\beta}$, $\boldsymbol{\zeta}$ and $\boldsymbol{\eta}$), and the problem can be efficiently solved. Likewise, if system parameters ($\boldsymbol{\alpha}$, $\boldsymbol{\beta}$, $\boldsymbol{\zeta}$ and $\boldsymbol{\eta}$) were known, Eq. (14) also becomes a convex optimization problem with variable $\boldsymbol{\psi}_{\mathrm{u}}$. Therefore, an iterative linearization procedure for efficiently solving the optimization problem is adopted in this study, similar to [3].

Figure 2 shows the pseudo code of the procedure. Each iteration step involves two operations, modal expansion and parameter updating. At each iteration, the first operation is essentially modal expansion for unmeasured DOFs $\boldsymbol{\psi}_{\mathrm{u}}$, where system parameters ($\boldsymbol{\alpha}$, $\boldsymbol{\beta}$, $\boldsymbol{\zeta}$ and $\boldsymbol{\eta}$) are from initial guess (starting values) for the first iteration step, or for later steps are from the updating results in the previous iteration. These parameters are thus constant in the first operation. The optimization problem over variables $\boldsymbol{\psi}_{\mathrm{u}}$ can be conveniently coded and efficiently solved using off-the-shelf solvers such as CVX [19]. The second operation at each iteration is the updating of model parameters ($\boldsymbol{\alpha}$, $\boldsymbol{\beta}$, $\boldsymbol{\zeta}$ and $\boldsymbol{\eta}$) using the expanded complete mode shapes from the first operation. Thus, $\boldsymbol{\psi}_{\mathrm{u}}$ is held as constant in the second operation. Again, off-the-shelf solvers such as CVX can be adopted to efficiently solve the optimization problem over variables ($\boldsymbol{\alpha}$, $\boldsymbol{\beta}$, $\boldsymbol{\zeta}$ and $\boldsymbol{\eta}$). Note that when Euclidean norm (2-norm) is adopted, the optimization problem without constraints is equivalent to a least square form for each operation and the detailed formulation can be found in [20].

## III. VALIDATION BY NUMERICAL SIMULATION OF A SPACE FRAME BRIDGE

To validate the proposed approach for substructure model updating, numerical model of a space frame bridge, which simulates a pedestrian bridge on Georgia Tech campus, is constructed. Figure 3 shows the space frame model containing 46 nodes, each node with six DOFs. Although mainly a frame structure, the segment cross bracings in top plane and two side planes are truss members. Transverse and vertical springs ($k_y$ and $k_z$) are allocated at both ends of the bridge to simulate non-ideal boundary conditions. In this study, it is assumed to have accurate information on structural mass; structural stiffness parameters are to be updated. TABLE I summarizes the structural stiffness parameters of the model. The parameters are divided into three categories. The first category contains six parameters (starting from top in the table), which are elastic moduli of the frame and truss (diagonal bracings in top plane) members along the entire length of the bridge. The second category contains ten parameters, which are the elastic moduli of truss members (diagonal bracings in two side planes) for different segments. The

```
start with α, β, ζ and η = 0 (meaning M and K start with M0 and K0) ;
REPEAT {
      (i) hold α, β, ζ and η as constant and minimize over variable ψu ;
      (ii) hold ψu as constant and minimize over variables α, β, ζ and η ;
} UNTIL convergence ;
```

Figure 2. Pseudo code of the iterative linearization procedure.

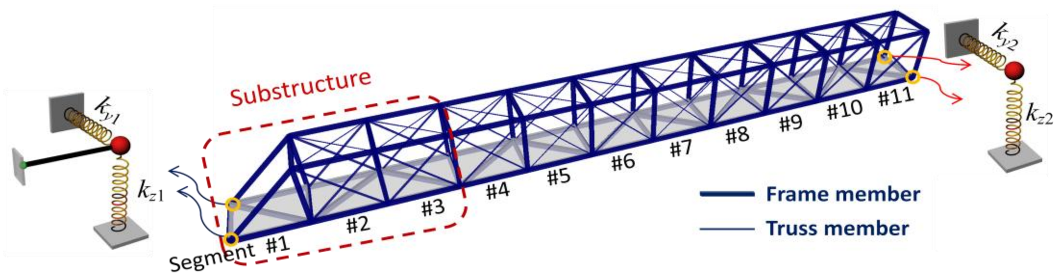


Figure 3. Substructure modeling of a space frame bridge.

TABLE I. STRUCTURAL STIFFNESS PARAMETERS

| Updating parameters | | | Initial value | Actual value | Change (%) |
|---|---|---|---|---|---|
| Elastic moduli of members along the bridge (kips/in$^2$) | Frame members | $E_1$ – Longitudinal top chord | 29,000 | 30,450 | 5 |
| | | $E_2$ – Longitudinal bottom chord | 29,000 | 30,450 | 5 |
| | | $E_3$ – Vertical members | 29,000 | 27,550 | -5 |
| | | $E_4$ – Transverse top chord | 29,000 | 30,450 | 5 |
| | | $E_5$ – Transverse & diagonal bottom chord | 29,000 | 30,450 | 5 |
| | Truss members | $E_6$ – Diagonal bracings in top plane | 29,000 | 27,550 | -5 |
| Elastic moduli of side-plane diagonal bracings (truss members) for each segment (kips/in$^2$) | $E_{S2}$ – 2$^{nd}$ segment | | 29,000 | 26,100 | -10 |
| | $E_{S3}$ – 3$^{rd}$ segment | | 29,000 | 26,100 | -10 |
| | $E_{S4}$ – 4$^{th}$ segment | | 29,000 | 26,100 | -10 |
| | $E_{S5}$ – 5$^{th}$ segment | | 29,000 | 27,550 | -5 |
| | $E_{S6}$ – 6$^{th}$ segment | | 29,000 | 27,550 | -5 |
| | $E_{S7}$ – 7$^{th}$ segment | | 29,000 | 27,550 | -5 |
| | $E_{S8}$ – 8$^{th}$ segment | | 29,000 | 24,650 | -15 |
| | $E_{S9}$ – 9$^{th}$ segment | | 29,000 | 26,100 | -10 |
| | $E_{S10}$ – 10$^{th}$ segment | | 29,000 | 27,550 | -5 |
| | $E_{S11}$ – 11$^{th}$ segment | | 29,000 | 27,550 | -5 |
| Support springs (kips/in) | $k_{y1}$ – Left transverse | | 200 | 140 | -30 |
| | $k_{z1}$ – Left vertical | | 500 | 800 | 60 |
| | $k_{y2}$ – Right transverse | | 200 | 140 | -30 |
| | $k_{z2}$ – Right vertical | | 500 | 800 | 60 |

third category contains stiffness parameters of the four types of support springs. TABLE I provides initial (nominal) values for all parameters, as starting point for model updating. The table also lists actual values, which ideally are to be identified. The relative changes from initial to actual values, to be identified, are also listed.

A substructure containing first three segments from left is selected for model updating (Figure 3). The selected substructure contains 10 substructure nodes and 4 interface nodes. Since each node has six DOFs and the longitudinal DOFs of the two support nodes are constrained, the substructure DOF vector is $\mathbf{x}_s \in \mathbb{R}^{58\times1}$ and the interface DOF vector is $\mathbf{x}_i \in \mathbb{R}^{24\times1}$. For practicality, it is assumed only translational DOFs of the substructure and interface nodes are instrumented with accelerometers for capturing substructure vibration modes; rotational DOFs are not measured. As described by formulation in Section II, no measurement is required on the residual structure. For model condensation, dynamic response of the residual structure is approximated using twenty modal coordinates, i.e. $n_q$ = 20 in Eq.(3). As a result, the entire structural model is condensed to $n_s+n_i+n_q$=102 DOFs (reduced from 274 DOFs in the original structure).

Since accurate structural mass matrix is assumed to be known, mass parameters $\boldsymbol{\beta}$ (Eq.(7)) is not among the updating parameters. Figure 4 shows the detailed view of the substructure containing the first three segments. The substructure stiffness parameters $\boldsymbol{\alpha}$ (being updated) include the five elastic moduli of the frame members ($E_1$~$E_5$), the elastic moduli of top bracing truss members ($E_6$), the elastic moduli of side-bracing truss members at the 2$^{nd}$ and 3$^{rd}$ segments ($E_{S2}$ and $E_{S3}$), and the spring stiffness values at the left support ($k_{y1}$ and $k_{z1}$). On the other hand, the residual structure is updated through modal parameters of the residual structure with free interface ($\zeta_2$, $\zeta_3$, ..., $\zeta_{44}$ and $\eta_1$, $\eta_2$, ..., $\eta_{44}$). Note that $n_i$+$n_q$ = 44 and that modal parameter $\zeta_1$ is not included. The reason is the first resonance frequency of the residual structure with free interface is zero (corresponding to free-body movement). As a result, the first modal correction matrix $\tilde{\mathbf{K}}_{R0,1}$ in Eq.(9) is a zero matrix, and so is the corresponding sensitivity matrix $\mathbf{S}_{\zeta,1}$. Using modal frequencies and substructure mode shapes ($\omega_j$ and $\boldsymbol{\psi}_{\mathrm{m},j}$) as "experimental data", the proposed modal dynamic residual approach is applied for substructure model updating. For each approach, the updating is

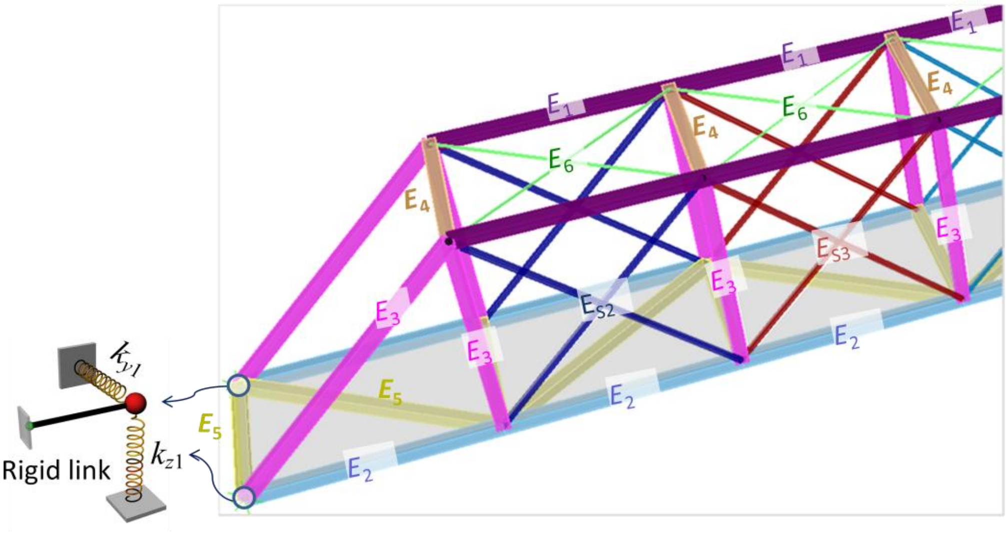


Figure 4. Detailed view of the substructure showing stiffness parameters to be updated.

performed assuming different numbers of measured modes are available (i.e. modes corresponding to the lowest three to six natural frequencies).

TABLE II summarizes the updating results using the proposed modal dynamic residual approach for substructure model updating. The results are presented in terms of relative change percentages from initial values. For every available number of modes, most of the updated parameter changes are close to the ideal percentages listed in TABLE I. The updating results for $E_4$, the elastic moduli of the transverse frame members in top plane are between -4.03% (with 6 modes) and -5.51% (with 3 modes). These results are most different from the actual/ideal change of +5%. The suspected reason is this parameter is less sensitive to translational DOFs. Another study shows if any rational DOF is measured, this parameter can be successfully updated. For clear demonstration of updating accuracy, Figure 5 plots the relative errors of the updating results, i.e. relative difference of updated values from the actual parameter values, for different number of available modes. The figure shows that except for $E_4$, the updating results accurately identify all other substructure stiffness parameters. In addition, the updating accuracy generally improves when more measured modes are available.

Although mostly small, updating errors do exist in this numerical example. The errors are mainly caused by the

TABLE II. UPDATED PARAMETER CHANGES (%) FOR SUBSTRUCTURE ELEMENTS BY MINIMIZATION OF MODAL DYNAMIC RESIDUAL

| **Number of available modes** | **Frame member** | | | | | **Truss member** | | | **Spring** | |
|---|---|---|---|---|---|---|---|---|---|---|
| | ***Longitudinal top ($E_1$)*** | ***Longitudinal bottom ($E_2$)*** | ***Vertical ($E_3$)*** | ***Transverse top ($E_4$)*** | ***Transverse bottom ($E_5$)*** | ***Top ($E_6$)*** | ***Side in 2nd segment ($E_{S2}$)*** | ***Side in 3rd segment ($E_{S3}$)*** | $k_{y1}$ | $k_{z1}$ |
| 3 modes | 3.41 | 2.94 | -6.35 | -5.51 | 2.90 | -6.60 | -11.48 | -12.00 | -31.42 | 57.63 |
| 4 modes | 4.81 | 4.23 | -5.03 | -4.38 | 4.21 | -5.23 | -10.33 | -10.76 | -30.55 | 59.83 |
| 5 modes | 4.93 | 4.36 | -5.02 | -4.40 | 4.33 | -5.82 | -10.20 | -10.98 | -30.47 | 59.92 |
| 6 modes | 4.96 | 4.38 | -4.97 | -4.03 | 4.36 | -6.34 | -10.19 | -12.39 | -30.42 | 59.98 |

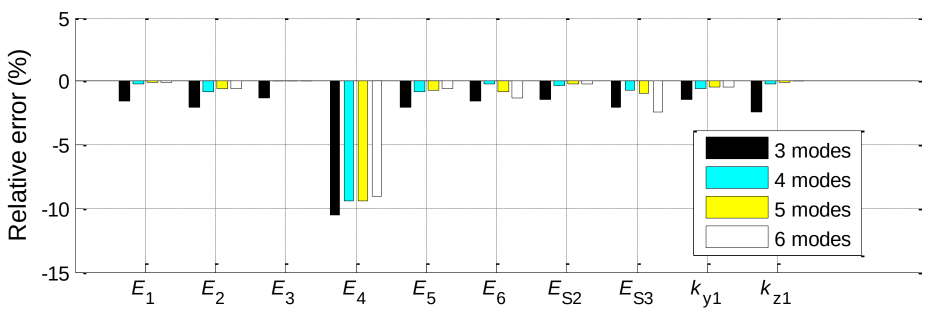


Figure 5. Relative errors of the updated parameters by minimization of modal dynamic residual

approximations made in the formulation for substructure model updating. First, the Craig-Bampton transform used in model condensation (Eq. (3)) adopts the static condensation matrix as the transformation matrix from interface DOFs to residual DOFs, which neglects interface dynamic contribution. Second, the Craig-Bampton transform uses only a few dominant modes describing dynamic behavior of the residual structure; higher-frequency modes are neglected. Third, while updating modal parameters for the residual structure, it is assumed that potential physical parameter changes in the residual structure do not significantly alter the generalized eigenvectors of the residual structural matrices (Eq.(8)). Nevertheless, the overall substructure updating performance through minimization of modal dynamic residual is reasonably accurate.

For comparison, substructure model updating is also performed using a conventional approach that minimizes experimental and simulated modal property differences [7]. The conventional model updating formulation aims to minimize the difference between experimental and simulated natural frequencies, as well as the difference between experimental and simulated mode shapes of the substructure.

$$\underset{\boldsymbol{\alpha},\boldsymbol{\beta},\boldsymbol{\zeta},\boldsymbol{\eta}}{\text{minimize}} \quad \sum_{j=1}^{n_m} \left\{ \left( \frac{\omega_j^{\text{FE}} - \omega_j}{\omega_j} \right)^2 + \left( \frac{1-\sqrt{\text{MAC}_j}}{\sqrt{\text{MAC}_j}} \right)^2 \right\} \tag{15}$$

where $\omega_j^{\text{FE}}$ and $\omega_j$ represent the $j$-th simulated (from the condensed model in Eq. (9) and (10)) and experimentally extracted frequencies, respectively; $\text{MAC}_j$ represents the modal assurance criterion evaluating the difference between the $j$-th simulated and experimental mode shapes. Note that mode shape entries only corresponding to measured DOFs are compared (i.e. between $\boldsymbol{\psi}_{\text{m},j}^{\text{FE}}$ and $\boldsymbol{\psi}_{\text{m},j}$). A nonlinear least-square optimization solver, ‘`lsqnonlin`’ in MATLAB toolbox [21], is adopted to numerically solve the optimization problem minimizing modal property differences. The optimization solver seeks a minimum through Levenberg-Marquardt algorithm, which adopts a search direction interpolated between the Gauss-Newton direction and the steepest descent direction [22].

TABLE III summarizes the updating results using the conventional approach minimizing modal property differences. Many of the updated/identified parameter changes are apparently different from the correct/ideal values listed in TABLE I. For clear demonstration of updating accuracy, Figure 6 plots the relative errors of the updating results. The figure shows that the updating results from conventional approach have much larger errors than the results from the proposed modal dynamic residual approach (Figure 5), particularly for support spring stiffness $k_{y1}$ and $k_{z1}$. The conventional approach minimizing modal property differences, when used for substructure model updating, cannot achieve a reasonable accuracy in this example. The main reason is that the objective function using modal property differences is not sensitive to minor changes in structural parameters. Moreover, the objective function using modal property differences is highly non-convex to structural parameters, so the optimization algorithm easily gets stuck at a local minimum.

TABLE III. UPDATED PARAMETER CHANGES (%) FOR SUBSTRUCTURE ELEMENTS BY MINIMIZATION OF MODAL PROPERTY DIFFERENCES

| **Number of available modes** | **Frame member** | | | | | **Truss member** | | | **Spring** | |
|---|---|---|---|---|---|---|---|---|---|---|
| | ***Longitudinal top ($E_1$)*** | ***Longitudinal bottom ($E_2$)*** | ***Vertical ($E_3$)*** | ***Transverse top ($E_4$)*** | ***Transverse bottom ($E_5$)*** | ***Top ($E_6$)*** | ***Side in 2nd segment ($E_{S2}$)*** | ***Side in 3rd segment ($E_{S3}$)*** | $k_{y1}$ | $k_{z1}$ |
| 3 modes | 2.65 | 6.19 | -3.88 | 3.51 | 4.34 | -4.53 | -9.05 | -7.42 | -0.12 | -0.13 |
| 4 modes | 3.05 | 6.76 | -5.34 | 5.99 | 2.09 | -6.96 | -9.05 | -10.19 | -0.87 | -0.19 |
| 5 modes | 5.35 | 13.53 | -0.09 | 0.66 | 1.9 | -0.58 | -4.09 | -3.75 | -0.29 | -0.01 |
| 6 modes | 7.71 | 17.92 | -0.73 | -1.02 | 8.04 | 4.26 | 2.42 | -6.24 | -0.62 | 0.03 |

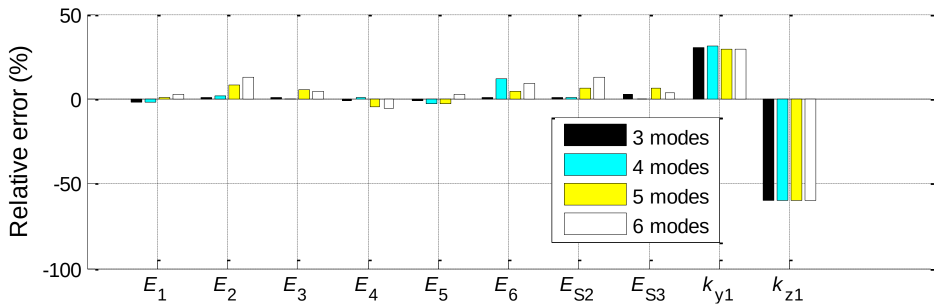


Figure 6. Relative errors of the updated parameters by minimization of modal property differences

## IV. Summary & Conclusion

This paper studies substructure model updating through minimization of modal dynamic residual. The entire structural model is divided into the substructure (currently being instrumented and to be updated) and the residual structure. Craig-Bampton transform is adopted to condense the residual structure using a limited number of dominant mode shapes, while the substructure remains at high resolution. To update the condensed structural model, physical parameters in the substructure and modal parameters of the residual structure are chosen as optimization variables; minimization of the modal dynamic residual is determined as the optimization objective. An iterative linearization procedure is adopted for efficiently solving the optimization problem.

The presented substructure updating method is validated through a space frame bridge example. About a quarter of the bridge is selected as the substructure being instrumented and updated. The proposed approach accurately identifies most of the parameters for the selected substructure. For comparison, a conventional approach minimizing modal property differences is also applied, but cannot achieve reasonable updating results. Future research will continue to investigate the substructure model updating approach on more complicated structural models, through both simulations and experiments.

## Acknowledgment

This research is sponsored by the National Science Foundation (#CMMI-1150700 and #CMMI-1041607), the Research and Innovative Technology Administration of US DOT (#DTRT12GUTC12) and Georgia DOT (#RP12-21). Any opinions, findings, and conclusions or recommendations expressed in this publication are those of the authors and do not necessarily reflect the view of the sponsors.

## References

[1] M. I. Friswell and J. E. Mottershead, *Finite element model updating in structural dynamics*. Dordrecht, Boston: Kluwer Academic Publishers, 1995.

[2] B. Jaishi and W. X. Ren, "Damage detection by finite element model updating using modal flexibility residual," *Journal of Sound and Vibration,* vol. 290, pp. 369-387, 2006.

[3] C. Farhat and F. M. Hemez, "Updating finite element dynamic models using an element-by-element sensitivity methodology," *AIAA Journal,* vol. 31, pp. 1702-1711, 1993.

[4] M. Hoshiya and E. Saito, "Structural identification by extended Kalman filter," *Journal of Engineering Mechanics-ASCE,* vol. 110, pp. 1757-1770, 1984.

[5] J. N. Yang, H. W. Huang, and S. W. Pan, "Adaptive Quadratic Sum-Squares Error for Structural Damage Identification," *Journal of Engineering Mechanics-Asce,* vol. 135, pp. 67-77, 2009.

[6] R. R. Craig, Jr. and M. C. C. Bampton, "Coupling of substructures of dynamics analyses," *AIAA Journal,* vol. 6, pp. 1313-1319, 1968.

[7] M. Link, "Updating analytical models by using local and global parameters and relaxed optimisation requirements," *Mechanical Systems and Signal Processing,* vol. 12, pp. 7-22, 1998.

[8] C. G. Koh and K. Shankar, "Substructural identification method without interface measurement," *Journal of Engineering Mechanics,* vol. 129, p. 769, 2003.

[9] Q. Zhao, T. Sawada, K. Hirao, and Y. Nariyuki, "Localized identification of MDOF structures in the frequency domain," *Earthquake Engineering & Structural Dynamics,* vol. 24, pp. 325-338, 1995.

[10] D. Zhang and E. A. Johnson, "Substructure identification for shear structures I: Substructure identification method," *Structural Control and Health Monitoring,* vol. 20, pp. 804-820, 2013.

[11] C. G. Koh, L. M. See, and T. Balendra, "Estimation of structural parameters in time domain - a substructure approach," *Earthquake Engineering & Structural Dynamics,* vol. 20, pp. 787-801, 1991.

[12] C. G. Koh, B. Hong, and C. Y. Liaw, "Substructural and progressive structural identification methods," *Engineering structures,* vol. 25, pp. 1551-1563, 2003.

[13] T. N. Trinh and C. G. Koh, "An improved substructural identification strategy for large structural systems," *Structural Control and Health Monitoring,* vol. 19, pp. 686-700, 2012.

[14] J. N. Yang and H. Huang, "Substructure damage identification using damage tracking technique," in *Proceedings of SPIE, Sensors and Smart Structures Technologies for Civil, Mechanical, and Aerospace Systems 2007*, San Diego, CA, USA, 2007, p. 65292R.

[15] K.-V. Yuen and L. S. Katafygiotis, "Substructure identification and health monitoring using noisy response measurements only," *Computer-Aided Civil and Infrastructure Engineering,* vol. 21, pp. 280-291, 2006.

[16] D. Zhu, X. Dong, and Y. Wang, "Substructure model updating through modal dynamic residual approach," in *Proceedings of the 9th International Workshop on Structural Health Monitoring*, Stanford, CA, 2013.

[17] D. Zhu and Y. Wang, "Substructure model updating through iterative convex optimization," in *Proceeding of the ASME 2012 Conference on Smart Materials, Adaptive Structures and Intelligent Systems (SMASIS 2012)*, Stone Mountain, GA, USA, 2012.

[18] S. P. Boyd and L. Vandenberghe, *Convex Optimization*. Cambridge, UK ; New York: Cambridge University Press, 2004.

[19] M. Grant and S. Boyd. (2014, Feb). *CVX: MATLAB software for disciplined convex programming, version 2.0*. Available: http://stanford.edu/~boyd/cvx.

[20] D. Zhu, X. Dong, and Y. Wang, "Substructure model updating through iterative minimization of modal dynamic residual," in *Proceedings of SPIE, Nondestructive Characterization for Composite Materials, Aerospace Engineering, Civil Infrastructure, and Homeland Security*, San Diego, California, USA, 2014.

[21] MathWorks Inc., *Control System Toolbox : for Uses with MATLAB® : Getting Started*, Version 6. ed. Natick, MA: MathWorks Inc., 2005.

[22] J. Moré, "The Levenberg-Marquardt algorithm: Implementation and theory," in *Numerical Analysis*. vol. 630, G. A. Watson, Ed., ed Berlin, Heidelberg, Germany: Springer, 1978, pp. 105-116.